NRIAG Journal of Astronomy and Geophysics (2015) 4, 205–221

National Research Institute of Astronomy and Geophysics

NRIAG Journal of Astronomy and Geophysics

www.elsevier.com/locate/nrjag

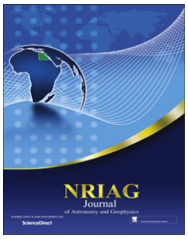

Earthquakes focal mechanism and stress field pattern in the northeastern part of Egypt

Emad K. Mohamed [a,*], **A. Hassoup** [a], **Abou Elenean K.M.** [a], **Adel A.A. Othman** [b], **Diaa-Eldin M.K. Hamed** [b]

[a] *National Research Institute of Astronomy and Geophysics (NRIAG), 11421 Helwan, Cairo, Egypt*
[b] *Faculty of Science, Al-Azhar University, Cairo, Egypt*

Received 20 July 2014; revised 3 September 2015; accepted 14 September 2015
Available online 23 October 2015

KEYWORDS

Seismicity;
Seismotectonics;
Focal mechanism;
Stress tensor inversion

Abstract Egypt is characterized by moderate size seismicity where earthquakes are distributed within several active regions. In the present study, we investigated the source mechanism of earthquakes using the digital waveform data recorded by the Egyptian National Seismic Network (ENSN) during the period from 2004 to 2008. The focal mechanisms are constructed with high reliability based on the polarity of the first motion of P-wave.

These solutions are used to examine the mode of tectonic deformation and the present-day stress field pattern affecting on different tectonic provinces in the northern part of Egypt. The results demonstrate mainly a normal faulting mechanism with minor strike slip component generally trending parallel to the northern Red Sea, the Suez rift, Aqaba rift with their connection with the great rift system of the Red Sea and the Gulf of Suez and Cairo-Alexandria trend.

The inversion technique scheme is used also in the present study for determining the regional stress field parameters for earthquake focal mechanism solutions based on the grid search method of Gephart and Forsyth (1984). The Results of the stress tensor using focal mechanisms of recent earthquakes show a prevailed tension stress field in N52°E, N41°E and N52°E for the northern Red Sea, Gulf of Suez and Gulf of Aqaba zone respectively.

1. Introduction

The northern part of Egypt is affected by tectonic movements along a number of plate tectonic boundaries. Thus, significant seismic activity is generated due to the relative motions between these three plates (African, Arabian and Eurasia plates). In this study, we focus on the area extending from 27°N to 31°N latitudes and 32°E to 36°E longitudes, which includes as few distinct regions (the Northern Red Sea, Gulf

* Corresponding author.
Peer review under responsibility of National Research Institute of Astronomy and Geophysics.

http://dx.doi.org/10.1016/j.nrjag.2015.09.001
2090-9977

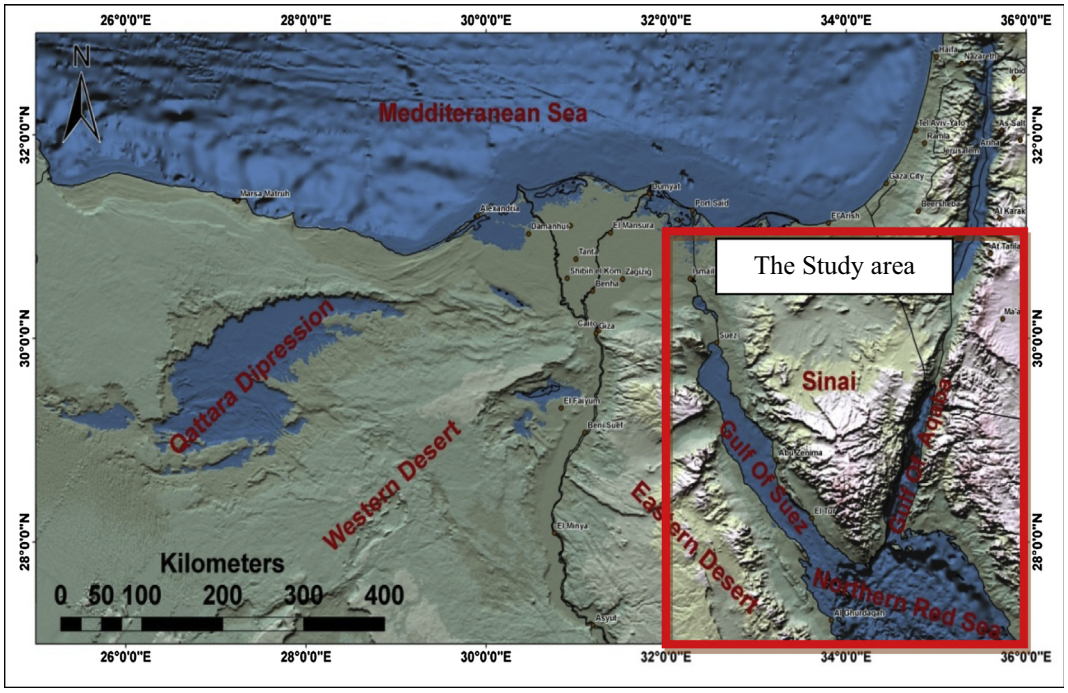

Figure 1 Location map of the study area.

of Suez, Gulf of Aqaba and Sinai Peninsula), as it is shown in Fig. 1.

The northern part of Egypt plays an important role in both historical and recent seismicity. Historically, few events have been reported very close to the Suez–Cairo district. The closer ones are that of 2200 BC (intensity = VII; macro seismic magnitude M_F = 5.4) and the destructive earthquake which occurred at the apex of the Suez Gulf in October, 1754 with intensity ranges ~VII–IX and M_F of 6.6 (Ambraseys et al., 1994). The large earthquakes are known to occur at larger distances along the northern Red Sea and the Gulf of Suez (e.g., the Shadwan earthquake in 1969 (M_W = 6.9); the Gulf of Aqaba earthquake in 1995 (M_W = 7.3) as well as in the Mediterranean offshore (i.e., the Alexandria earthquake in 1955 (M_S = 6.8); and the Cyprus earthquake in 1996 (M_W = 6.8). Instrumental seismicity from November 1997 to December 2009 shows few small-moderate size events with magnitudes up to M_L = 5 in this active area that are well recorded by the Egyptian National Seismic Network (ENSN) Bulletin (1997–2009).

There are several methods used for determining focal mechanism solutions (FMSs) such as polarity of P-wave first motion, amplitude ratio of S waves (e.g. Khattri, 1973), the analysis of P/S amplitude ratios (e.g. Kisslinger et al., 1981) and moment tensor inversion (e.g., Stein and Wysession, 2003). All these methods used the radiation pattern of seismic rays that expresses the orientation of the active fault and the slip direction.

In the present study we determined the focal mechanism solutions based on the polarity of P-wave first motion where constructed for a set of earthquakes that occurred during the period 2004–2008 in order to evaluate the stress field pattern affecting on the area of study using the digital waveform data recorded by the Egyptian National Seismic Network (ENSN) Fig. 2.

Knowledge of the stress field in a region is an important tool to understand local and regional effects induced by large-scale plate tectonics and the subsequent deformation field. According to the objects used to retrieve the stress field, different time periods are sampled. On one hand, slickensides measured on a sedimentary or crystalline outcrop describe the whole tectonic history experienced by the region. On the other hand, seismological data give an instantaneous picture of the present-day stress field. For example, Lund and Slunga (1999) presented stress tensor inversion based on detailed micro-earthquakes data in southwest Iceland. Together with accurate relative location, it was possible to assign a common fault plane to a cluster of events. In this paper, the direction and the shape of the stress tensor in the Northern Red Sea, Gulf of Suez and Gulf of Aqaba were determined from the seismological data, providing us with the present-day average state of stress prevailing in the region.

2. Geological and tectonic setting

The Study area is a part of the northern African continent. Egypt forms the northeast corner of Africa and is bounded by three active tectonic margins: the African–Eurasian plate margin; the Red Sea plate margin; and the Levant-Dead Sea transform fault. Three main tectonic deformations affecting northern Egypt are Jurassic-Early Cretaceous rifting, Late Cretaceous-Early Tertiary wrenching, and Miocene and post-Miocene extension. The tectonics of northern Egypt has been developed depending on detailed subsurface studies of the authors (Abdel Aal et al., 1994; Mosconi et al., 1996). Generally the major part of tectonic deformation within Egypt is remote and took place along those margins mentioned before (the African–Eurasian plate margin; the Red Sea plate margin; and the Levant-Dead Sea transform fault) as revealed by an

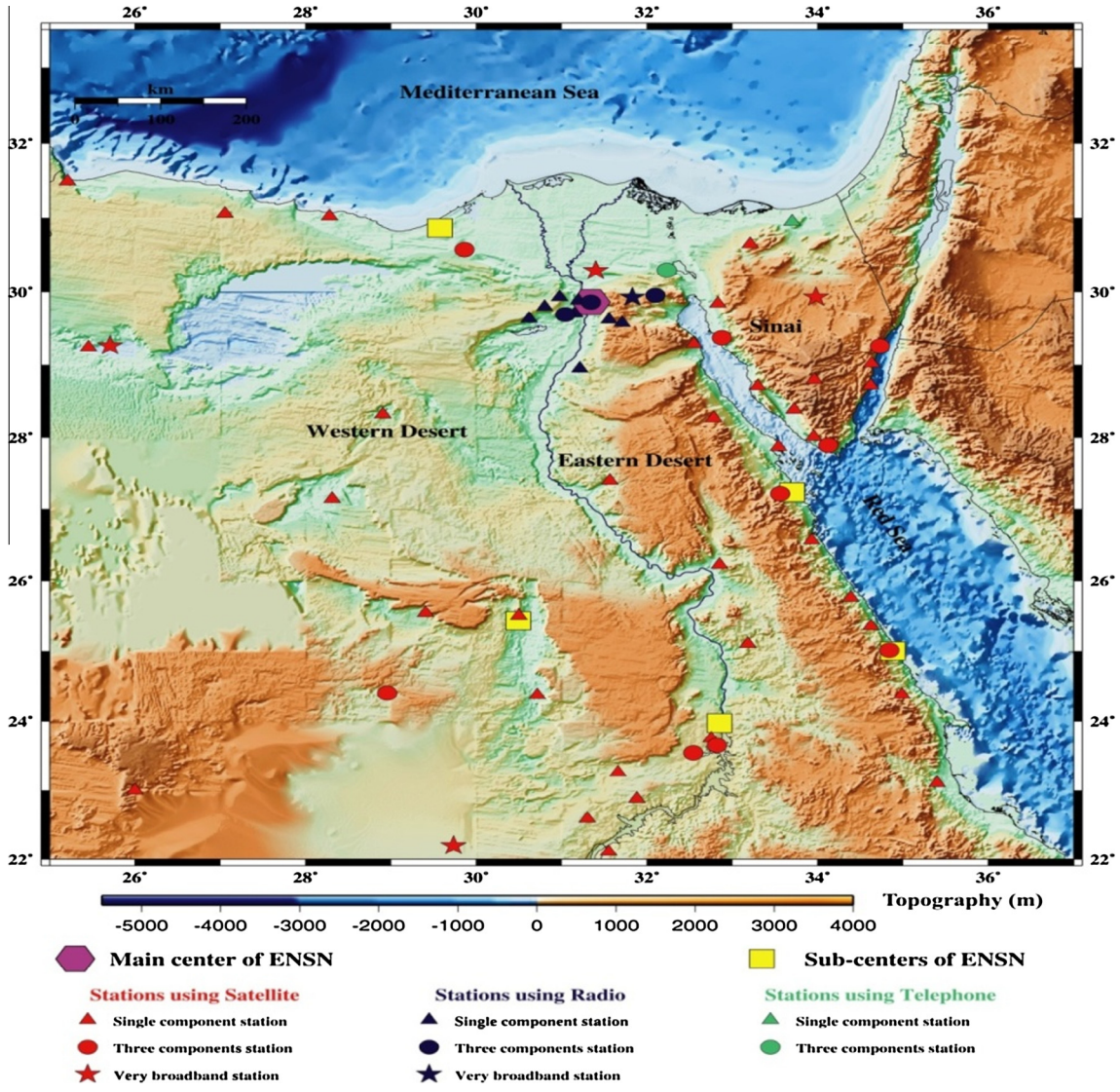

Figure 2 Geographic distribution of Egyptian National Seismic Network (ENSN) Stations.

observed highest rate of the seismic activity. Basing on geophysics studies in the territory of Egypt, three major tectonic trends are recognized namely the Red Sea trend oriented NW-SE, the Gulf of Aqaba trend oriented NE-SW and the Mediterranean trend oriented E-W (Youssef, 1968). On the other hand, Halsey and Gardner (1975) and Meshref (1982) considered the WNW-ESE trend as the significant tectonic trend in northern Egypt.

The Gulf of Suez is northwest trending basin stretches some 300 km north by northwest, separated from the Red Sea by the Aqaba transform fault, terminating at Suez city at the southern entrance of the Suez Canal. The major features of forces are the existence of a series of major faults that extend along the rift and bound it from both sides in Fig. 3. Meshref (1990) excluded the rifting by right lateral but approved a regional extension in a direction approximately perpendicular to it. The present shape of the Gulf of Suez has been determined by fracture systems which were possibly still due to tectonic events caused by movements of the Nubian, Arabian and Sinai plates and also the resulting rift trend, the (NNE-SSW) Aqaba trend.

The Red Sea, which forms the boundary between the African plate and Arabian plate, bifurcates into two branches: the Gulf of Suez and the Gulf of Aqaba. The Red Sea includes extensive shallow shelves, which were formed by Arabia splitting from Africa due to plate tectonics. The northern Red Sea is characterized by active extensional features (Ben-Menahem et al., 1976) and it occupies an elongated escarpment bounded depression between the uplifted Arabian and Nubian Shields. Stratigraphic and structural studies show that the Red Sea and Gulf of Suez rifting began in Oligocene time and developed in Miocene (Garfunkel and Bartov, 1977).

The Gulf of Aqaba represents the arm of the Red Sea, separating Saudi Arabia and Sinai Peninsula and its main faults trends are in the N-S to NNE-SSW directions. The Gulf of Aqaba formed the inner, active core of a 60–80 km wide deformation zone that constitutes the southern segment of Dead Sea Transform (DST). Eyal et al. (1981) and (Garfunkel and

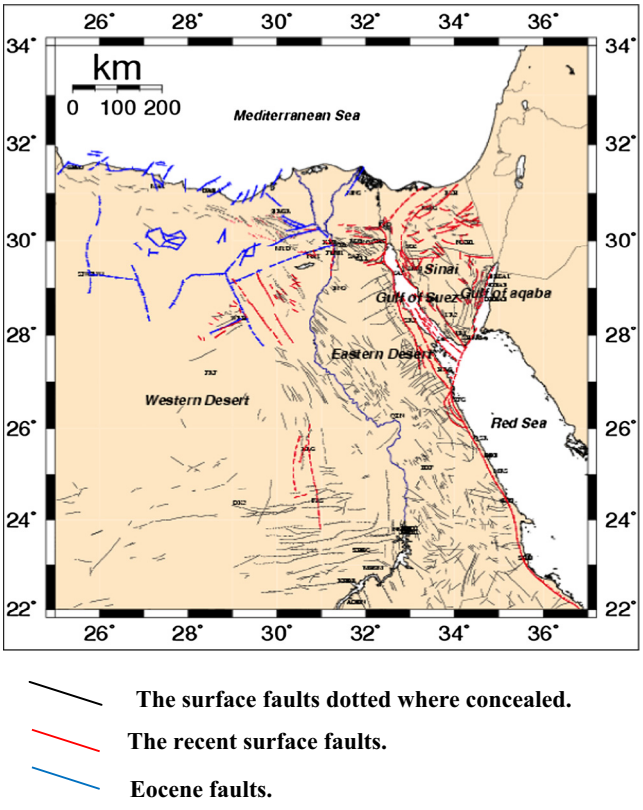

Figure 3 Tectonic boundaries of the Eastern Mediterranean Region (compiled by Abou Elenean and Hussein (2008) and Egyptian Geological Survey (1981)).

Ben-Avraham, 1996) returned back to the late Oligocene and early Miocene nearly at the initial stage of the Red Sea rift, also they produced an independent estimation of the total motion is about 100 km from regional plate kinematics data. The Gulf of Aqaba is narrow structure and characterized by significant depths reaching 1800 and surrounding by high mountain range of Sinai and Hejaz up to 2600 m; therefore, the total difference in height over 4000 m suggested that tectonic processes have occurred faster than erosive processes (Klinger et al., 1999). From the field studies, Lyberis (1988) and Bayer et al. (1988) observed two conjugate faults along the Gulf of Aqaba; NNE left lateral strike slip faults parallel to the gulf that release the majority of stress and nearly ESE-WNW normal faults along the margins of pull apart basins. Furthermore, Pinar and Türkelli (1997), Klinger et al. (1999), Hofstetter et al. (2003), Abdel Fattah et al. (2006) asserted the dominance of ENE-WSW extension (N60°-80°E) along the Gulf of Aqaba.

3. Data and methods

The waveform data (Seismograms) used in the present study were obtained mainly from the National Seismic Network in Egypt (ENSN) which established in 1997, Fig. 1. These data are extracted from remote sites online to the ring buffer by ATLAS PROGRAM Version 1.2 Fig. 4, provided by Nanometrics Inc., Kanata, Ontario (Canada). The stations from other neighboring networks are generally too far from the epicenter of the earthquakes to provide useful information, and thus, only a few data readings of those networks were incorporated in our data set such as Elat Station in Israel.

A re-location for 24 selected seismic events during the period from 2004 to the end 2008 was done using HYPOINVERSE Program. Events which fulfilled the following conditions were selected and the conditions are at least very clear 10 P-wave phases and at least 2 S-wave very clear phases, good azimuth coverage of stations and keeping only events with low RMS. The second step is to check the number and the coherency of the polarities; hence, the focal mechanisms were constructed.

The focal mechanisms of events have been done manually to test and avoid earthquakes with noticeable wrong polarities.

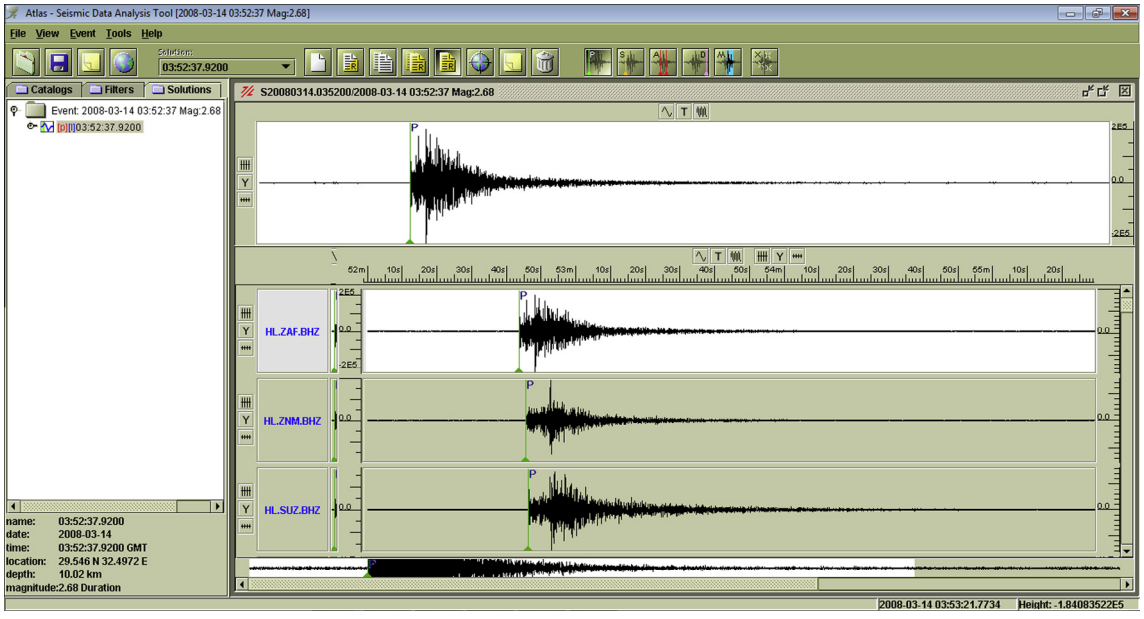

Figure 4 An example of picking of P-wave phases using ATLAS Software.

Table 1 Crustal structure models used for different regions.

Layer No.	First layer			Second layer			Third layer			Fourth layer		
Layer parameters	H	Vp	Vs	H	Vp	Vs	H	Vp	Vs	H	Vp	Vs
El-Hadidy (1995)	3.5	4.5	2.52	12.5	6	3.37	15	6.5	3.6	–	8.0	4.49
Marzouk (1988)	4.0	4.0	2.32	8.0	6.3	3.66	10	6.6	3.83	–	8.0	4.47

Abbreviations: H: layer thickness; Vp: P-wave velocity; Vs: shear wave velocity.

The solutions are carried out using the software package developed by Suetsugu (1995). Two-dimensional P-wave velocity models El-Hadidy (1995) for Gulf of Suez and Gulf of Aqaba area, and (Marzouk, 1988) for Northern Red Sea were used for locating the studied events as shown in Table 1. In our study we used the grid search method of Gephart and Forsyth (1984) for determining the orientation and shape of the stress tensor.

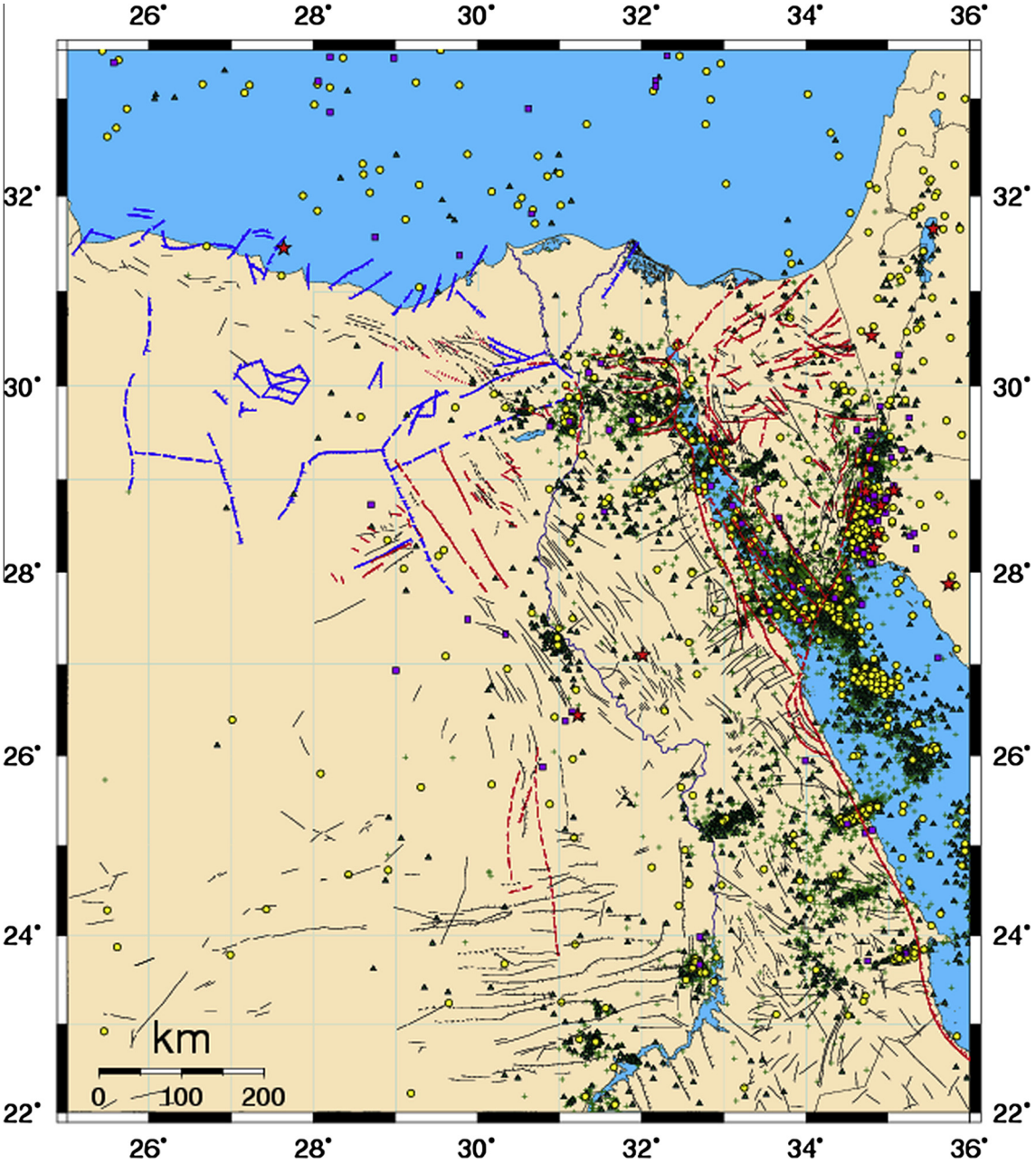

Figure 5 Local Seismic activity recorded by Egyptian National Seismic Network (ENSN) during the period from November, 1997 to December 2008.

4. Seismicity

The seismicity of Egypt was studied by many authors (e.g., Sieberg, 1932; Ismail, 1960; Gergawi and El-Khashab, 1968; Maamoun et al., 1984; Kebeasy, 1990; Abou Elenean, 1997). In their studies, the seismicity maps are based on the regional geological structures and sometimes based on the dominant tectonic stress. The seismic activity was reported in four narrow belts (Levant-Aqaba; Northern Red Sea-Gulf of Suez; Cairo–Alexandria trend; Eastern Mediterranean–Cairo–Fayoum and Mediterranean Coastal Dislocation) which represent the major tectonic trends in northern Egypt.

The seismicity of Egypt was characterized by small to moderate earthquakes due to the relative motions between the African, Arabian and Eurasian plates. The highest seismicity rates are found at the eastern boundaries of Egypt at the Gulf of Aqaba which forms the southern end of the Dead Sea Fault and the northern part of the Red Sea.

With the establishment of Egyptian National Seismic Network (ENSN) more activity with accurate parameters was revealed. The earthquakes recorded by ENSN from November 1997 to December 2009 reflected incredible increase in the number of smaller earthquakes. This large number of events could be attributed to the increase of the seismic stations and hence the delectability of ENSN. These earthquakes are located at specific seismic zones that reflect their tectonic activity for local and regional events in Figs. 5 and 6 respectively which are as follows:

1. Cairo-Suez shear zone which extends from the apex of the Suez Gulf toward Cairo City and is characterized by moderate activity.

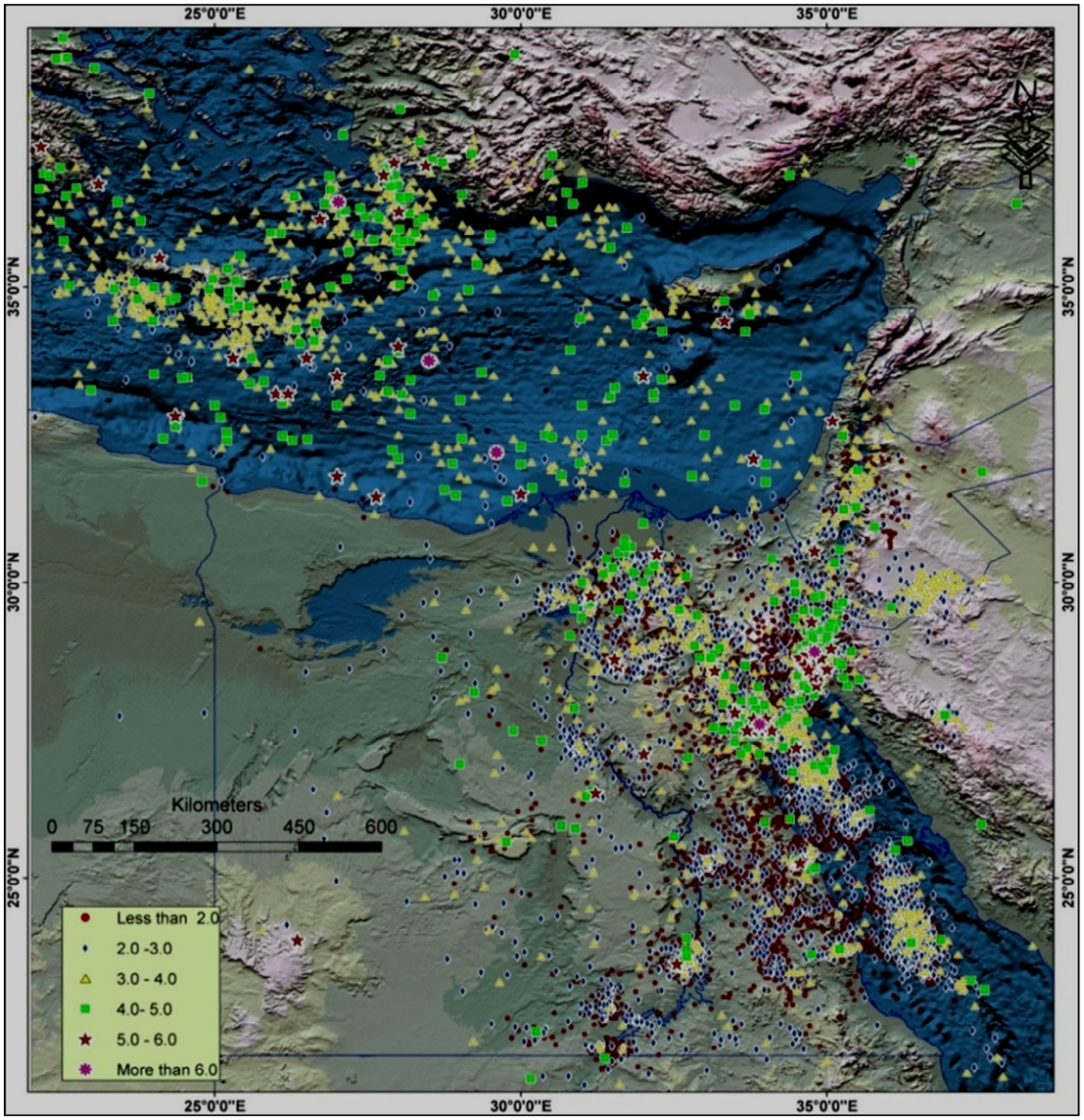

Figure 6 The compiling of local and regional seismic activity recorded by Egyptian National Seismic Network from November, 1997 to December 2009 (modified after Abou Elenean and Hussein, 2008; Egyptian Geological Survey, 1981).

2. The Gulf of Aqaba and its extension toward into the north which is characterized by high seismic activity.
3. The entire Gulf of Suez a cluster of seismic activity comes clearly from the central part of Gulf.
4. The northern part of the Red Sea characterized by seismic activity which tends to lie at the Aqaba fault extension to the south.

5. Focal mechanism

Focal mechanisms of small to moderate size earthquakes recorded by ENSN indicate a Normal faulting with strike slip component and these fault plane solutions correspond to active faults of each area and prevailing dominant tension stress along the northeast African corner and a dominant compression toward the Mediterranean Sea along the transition zone between the continental and oceanic crusts. The tension axis trends ENE-WSW along the Gulf of Suez, Gulf of Aqaba, and the Red Sea rift. The following are the results of focal mechanism solutions for each active zone.

5.1. The northern Red Sea

In this study thirteen events are selected. The location of these events is shown in Fig. 7 and the hypocentral parameters of these events and focal mechanism parameters are listed in Table. 2. These solutions are subdivided into three groups. The first group is located at the entrance of Gulf of Aqaba Fig. 7. The event no. 3 located at the Gulf of Aqaba entrance shows a strike slip faulting with minor normal component and its nodal planes are trending nearly NNE-SSW and ESE-WNW, while the event no. (6, 7, 12, 13) show mainly normal faulting, their nodal planes are trending N-S to NW-SE parallel to the Red Sea rift axis and its extension along the Suez gulf. These events show a *T*-axis directed NE-SW, which is consistent with the dominant tension stress along the Red Sea.

The second group is located at the south tip of Sinai Fig. 7: events no. (1, 5, 9, 11) show a normal faulting mechanism with minor strike slip components and its nodal planes trending NW-SE to N-S and all planes are nearly parallel to the Red Sea trend except event no. (1), its nodal planes trending NW-SE to E-W.

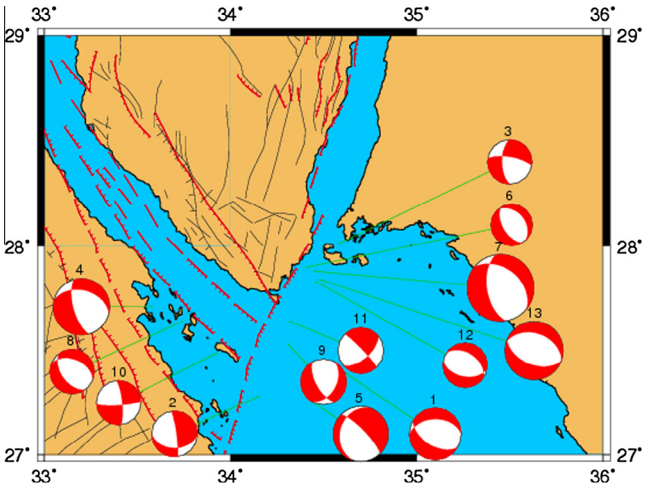

Figure 7 The location of the events used for focal mechanism analysis in the northern Red Sea. The numbers above the focal mechanism are their orders according to Table 2.

The third group is located at Shadwan Island and surrounding area, Fig. 7: event no. (10) that is located at Shadwan Island shows strike slip faulting with nodal planes trending N-S and E-W. This event is located very close to the proposed site of the triple junction (Red Sea–Gulf of Suez–Gulf of Aqaba) while events no. (2, 4 and 8) located at the entrance of the Suez gulf show normal faulting with strike slip components but event no. (10) Close to Shadwan Island shows Strike slip fault with normal components. The Planes of the events no. (4 and 8) are directed parallel to both Gulf of Suez and the Red Sea.

All focal mechanism solutions gave a *T*-axis directed ENE-WSW which is consistent with the dominant tension stress along both Gulf of Suez and the Red Sea according to Previous studies (Abou Elenean, 1997; Megahed, 2004), and they suggested that the focal mechanisms along the northern Red

Table 2 The source parameters of events located at the northern Red Sea.

No.	Date			Time			Location		Nodal plane			H (km)	RMS	ERH	ERZ	ML
	Y	M	D	H	M	S	Lat.	Long.	Strike	Dip	Rake					
1	2004	04	27	11	20	40	27.39	34.62	121	52	−69	5.5	0.3	1.54	3.9	3.5
2	2005	05	04	19	47	15	27.28	34.15	352	83	−52	5.4	0.1	1.87	14.93	3.1
3	2005	07	23	14	55	22	28.01	34.58	179	61	−22	5.5	0.1	2.5	3.4	3.0
4	2005	10	28	17	00	09	27.71	33.58	284	41	−143	25	0.16	1.0	1.57	3.8
5	2005	11	11	15	33	08	27.26	34.43	196	25	−32	11	0.0	2.5	3.8	3.7
6	2006	01	30	03	33	27	27.90	34.41	149	55	−84	15	0.21	1.22	1.09	2.8
7	2006	02	02	09	49	50	27.88	34.45	309	41	−124	12	0.29	0.84	1.32	4.5
8	2006	04	06	10	58	12	27.64	33.74	144	50	−68	9.3	0.20	1.27	2.54	3.0
9	2008	03	20	09	06	33	27.53	34.31	151	63	−126	7.49	0.28	2.61	3.01	3.1
10	2008	05	04	01	08	15	27.49	33.93	354	77	−10	3.9	0.20	0.70	2.13	3.0
11	2008	05	24	00	37	53	27.64	34.32	316	84	−31	4.0	0.20	1.14	2.01	3.1
12	2008	05	29	06	10	50	27.83	34.46	304	44	−73	7.1	0.22	1.03	2.27	3.0
13	2008	05	29	07	16	22	27.84	34.48	289	40	−92	8.1	0.24	0.93	2.22	3.9

ML: local magnitude, H: focal depth, RMS: root mean square, ERH: error in horizontal direction, ERZ: error in vertical.

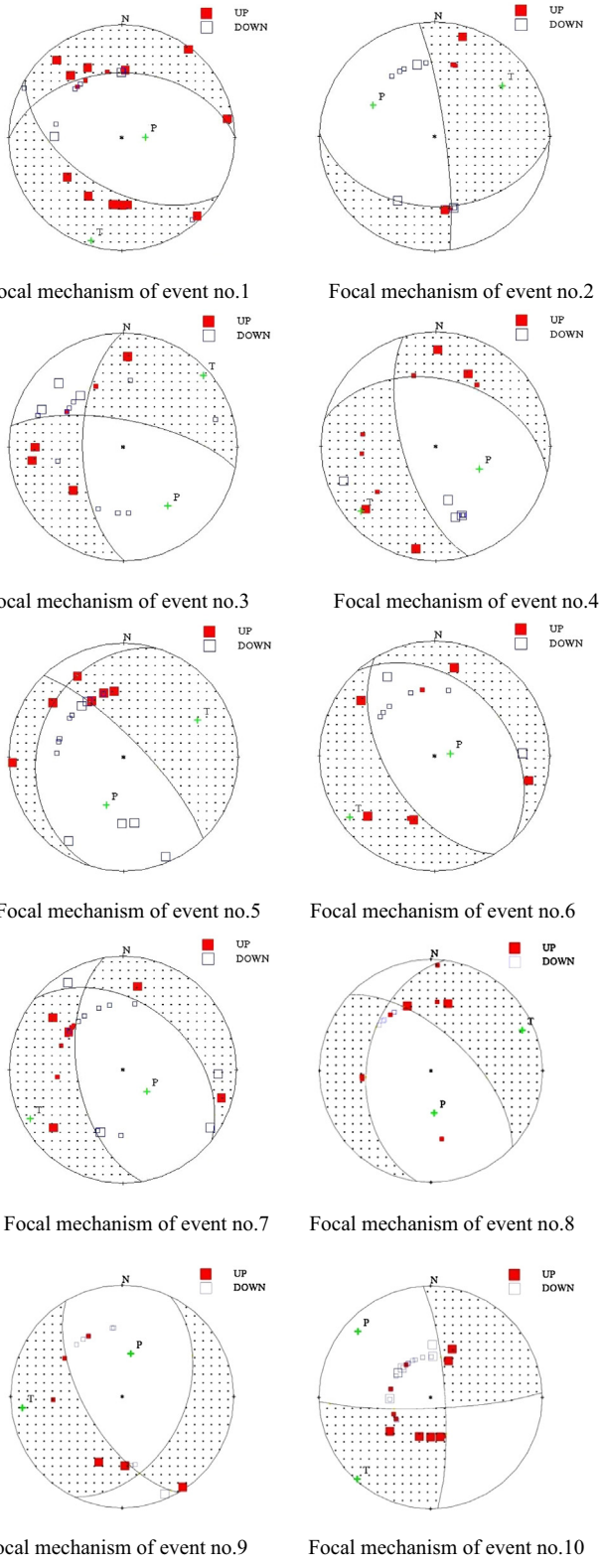

Focal mechanism of event no.1 Focal mechanism of event no.2

Focal mechanism of event no.3 Focal mechanism of event no.4

Focal mechanism of event no.5 Focal mechanism of event no.6

Focal mechanism of event no.7 Focal mechanism of event no.8

Focal mechanism of event no.9 Focal mechanism of event no.10

Figure 8 Diagrams of focal mechanism solutions of events located at the northern Red Sea.

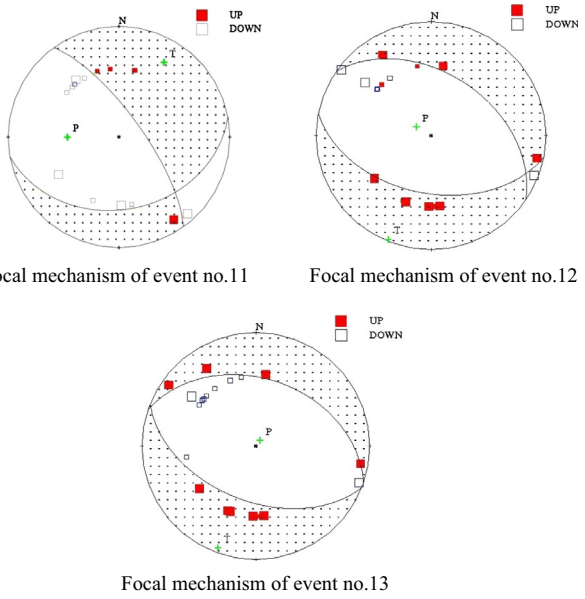

Focal mechanism of event no.11 Focal mechanism of event no.12

Focal mechanism of event no.13

Fig. 8 (*continued*)

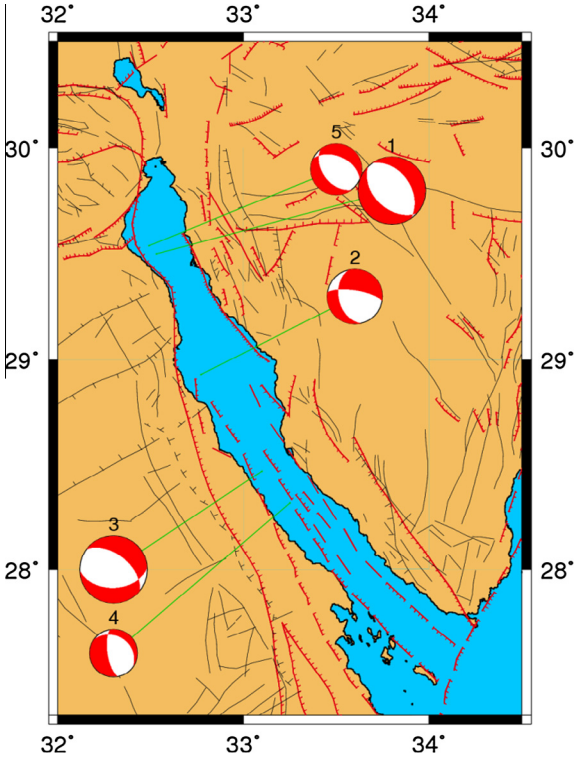

Figure 9 The location of the events used for focal mechanism analysis in the Gulf of Suez. The numbers above the focal mechanism are their orders according to Table 3.

Sea-southern part of Suez gulf have a dominant ENE-WSW tension stress (~N56°E) with the exception of local stress perturbation closer to the proposed triple junction. Fig. 8 shows diagrams of focal mechanism solutions of each event located at the northern Red Sea. In this paper, some data are not enough to define the two planes due to lack of stations and are well not distributed geographically around the epicenter, e.g. events no. (2, 8 and 9).

Table 3 The source parameters of events located at the Gulf of Suez.

No.	Date			Time			Location		Nodal Plane			H (km)	RMS	ERH	ERZ	ML
	Y	M	D	H	M	S	Lat.	Long.	St.	Dip	Rake					
1	2004	07	06	12	13	15	29.50	32.53	325	44	−82	24.4	0.3	1.21	1.55	3.4
2	2004	08	16	22	42	50	28.93	32.77	279	72	−128	8.4	0.2	1.66	2.5	2.8
3	2006	09	28	06	32	12	28.47	33.10	308	53	−63	13.5	0.2	0.59	1.24	3.4
4	2008	01	25	03	19	42	28.32	33.25	304	30	−133	17.5	0.1	1.03	2.07	2.4
5	2008	03	14	03	52	37	29.54	32.49	143	46	−69	10.0	0.1	0.72	0.83	2.6

ML: local magnitude, H: focal depth, RMS: root mean square, ERH: error in horizontal direction, ERZ: error in vertical.

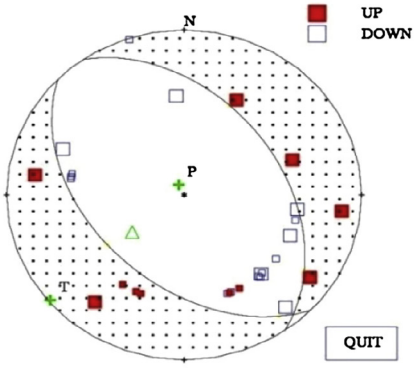

Focal mechanism of event no.1

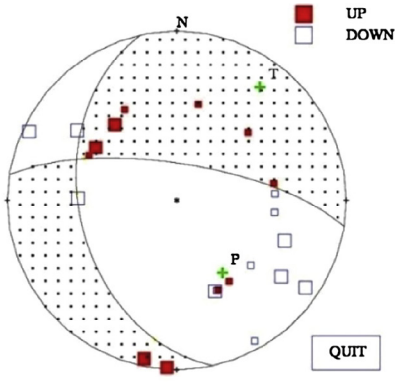

Focal mechanism of event no. 2

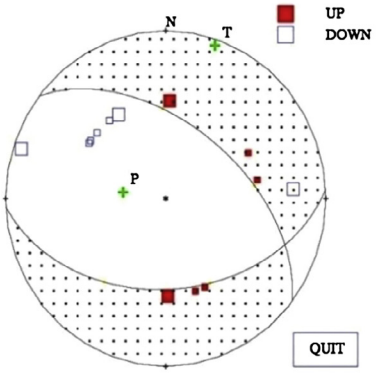

Focal mechanism of event no. 3

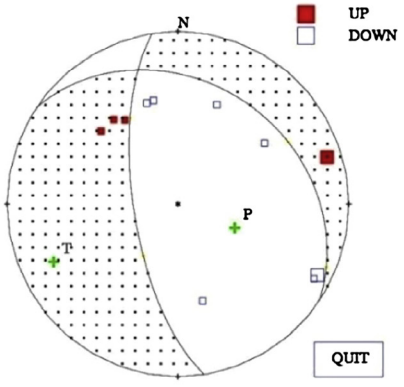

Focal mechanism of event no. 4

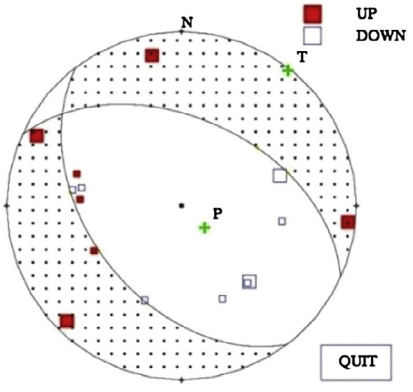

Focal mechanism of event no. 5

Figure 10 Diagrams of focal mechanism solutions of events located at the Gulf of Suez.

5.2. The Gulf of Suez

In this area five earthquakes are selected for focal mechanism analysis. The solutions of events no. 1, 3, 5 are mainly pure normal faulting mechanism and its nodal planes trending NW-SE and parallel to the Gulf but event no. 2 is trending NW-SE and N-S and event no. 4 is trending NW-SE and E-W. These solutions reflect good agreement with the surface faults crossing the Eastern Desert from the Gulf apex toward Cairo as shown in Fig. 9 and their parameters are listed in Table 3. They occurred along the central part of the Gulf of Suez and reflected generally normal fault that has the main trend of the Suez Gulf. The dominant tension stress prevails along the entire Suez Gulf without an indication of compressive stress.

Previous studies along The Gulf of Suez illustrated that there is a left lateral movement (Ben-Menahem and Aboodi, 1971; Ben-Menahem et al., 1976; Garfunkel and Bartov, 1977; Chenet et al., 1985), while Maamoun et al. (1980), Tapponnier and Armijo (1985), Courtillot et al. (1987), Moustafa and Abd-Allah (1992) and Moustafa (2002) assumed a right lateral movement. The Focal mechanism solutions along the Gulf of Suez in this study reveal slight right lateral shear along WNW-ESE. All rupture planes are directed parallel to the gulf, and the main trend of *T*-axis from all solutions along the gulf is NNE-SSW which is consistent with the dominant tension stress along the Gulf of Suez. Fig. 10 shows diagrams of focal mechanism solution of each event located at the Gulf of Suez.

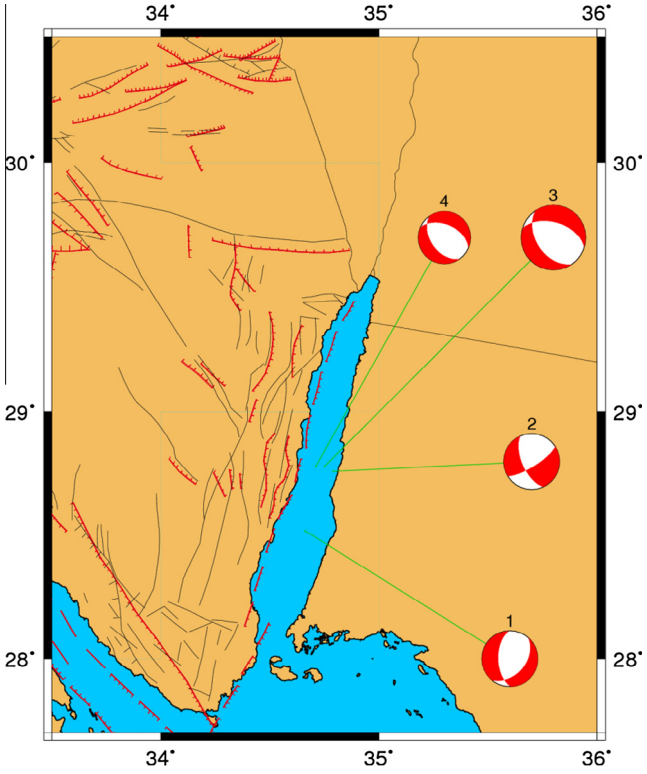

Figure 11 The location of the events used for focal mechanism analysis in the Gulf of Aqaba. The numbers above focal mechanism are their orders according to Table 4.

5.3. The Gulf of Aqaba

The Gulf of Aqaba is the most active seismic source in Egypt, many of its recorded events are not considered due to either the lack of data or the bad azimuth cover of the ENSN along the Gulf of Aqaba. Only four events at the central part are selected. The solutions of the events are shown in Fig. 11 and their parameters are listed in Table 4. The solution of events no. 3 and 4 close to each other with the same location shows normal faults with minor strike slip components along nodal planes trending NW-SE and WNW-ESE. These planes are consistent with the transverse faults crossing the main Aqaba fault trends. These events gave *P*-axis directed NW-SE and *T*-axis directed NE-SW which is consistent with the dominant tension stress along Gulf of Aqaba.

Meanwhile, the solutions of events no. 1 and 2 show also normal faults with larger strike slip components along nodal planes trending nearly NNE-SSW parallel to the main Aqaba trend. The *P*-axis of these events is directed NE-SW while the *T*-axis is directed nearly E-W perpendicular to the Gulf of Aqaba.

Many authors (Pinar and Türkelli, 1997; Klinger et al., 1999; Hofstetter et al., 2003; Abdel Fattah et al., 2006) assert the dominance of ENE-WSW extension (N60°-80°E) along the Gulf of Aqaba. Furthermore, from the field studies (Lyberis, 1988 and Bayer et al., 1988) observed two conjugate faults along the Gulf of Aqaba; NNE left lateral strike slip faults parallel to the Gulf that release the majority of stress and nearly ESE-WNW normal faults along the margins of pull apart basins. Fig. 12 shows diagrams of focal mechanism solution of each event located at the Gulf of Aqaba.

5.4. Sinai Peninsula

Only two events are selected in this area due to the fact that the occurrences of moderate size earthquakes were fewer during our study time interval. Also, the most of this area located

Table 4 The source parameters of events located at the Gulf of Aqaba.

No.	Date			Time			Location		Nodal Plane			H (km)	RMS	ERH	ERZ	ML
	Y	M	D	H	M	S	Lat.	Long.	St.	Dip	Rake					
1	2005	01	20	13	41	50	28.50	34.66	41	43	−56	18.78	0.3	2.93	1.48	3.2
2	2008	02	03	17	06	46	28.76	34.79	58	75	−29	13.69	0.2	1.65	0.69	3.2
3	2008	04	04	14	05	20	28.78	34.75	146	46	−61	6.87	0.3	2.52	1.51	3.7
4	2008	04	04	14	14	48	28.70	34.71	145	46	−67	7.11	0.2	2.21	1.31	3.0

H: focal depth, RMS: root mean square, ERH: error in horizontal direction, ERZ: error in vertical.

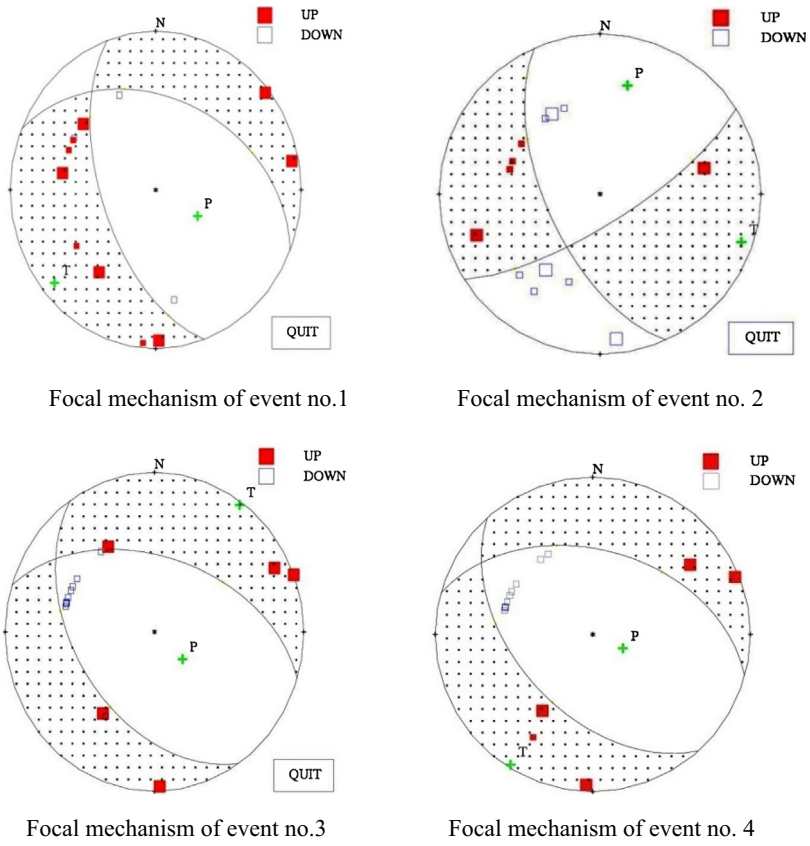

Figure 12 Diagrams of focal mechanism solutions of events located at The Gulf of Aqaba.

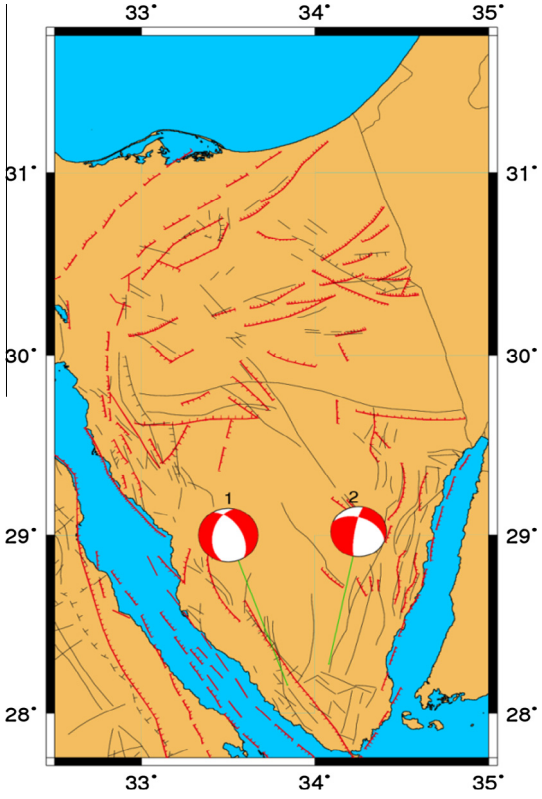

Figure 13 The location of the events used for focal mechanism analysis in Sinai Peninsula. The numbers above focal mechanism are their orders according to Table 5.

at the stable shelf. Hence it is characterized by low seismicity. The focal mechanisms of these events show normal faults with minor strike slip components in Fig. 13, their parameters are listed in Table 5 and their nodal planes are trending NW-SE and NNE-SSW, parallel to both northern Red Sea and Suez Gulf trends. Fig. 14 shows diagrams of focal mechanism solutions of each event located at Sinai Peninsula.

6. Stress tensor inversion

In the stress inversion analysis, it is assumed that during the faulting process of the upper crust, a set of invariant geometrical properties emerges whose most obvious expression is the Gutenberg and Richter law (De Vicente et al., 2006). From this point of view, it is possible to carry out the inversion without taking into account, or to scale, the focal mechanisms according to its magnitude. In the same way, there is not a minimum representative magnitude of the state of the tectonic stresses, so the only applied criterion is that of solution quality.

The analysis of earthquakes focal mechanism using inversion methods allows determining the state of active stress; therefore, in this study we used Gephart and Forsyth (GF) method (1984) which allows us to determine the best-fit regional principal stress directions $\sigma 1$, $\sigma 2$, and $\sigma 3$ and the ratio $R = \sigma 2 - \sigma 1/\sigma 3 - \sigma 1$ with F (the average degree of misfit), as well as to estimate the associated uncertainty in the solution. The value of the ratio R is a measure of the magnitude of the intermediate principal stress $\sigma 2$ relative to the maximum $\sigma 1$

Table 5 The source parameters of events located at Sinai Peninsula.

No.	Date			Time			Location		Nodal plane			H (km)	RMS	ERH	ERZ	ML
	Y	M	D	H	M	S	Lat.	Long.	St.	Dip	Rake					
1	2008	06	26	23	25	25	28.16	33.84	192	46	−57	4.57	0.25	0.88	1.32	3.2
2	2008	12	28	09	36	34	28.28	34.08	190	79	−46	18.07	0.16	0.71	0.77	3.0

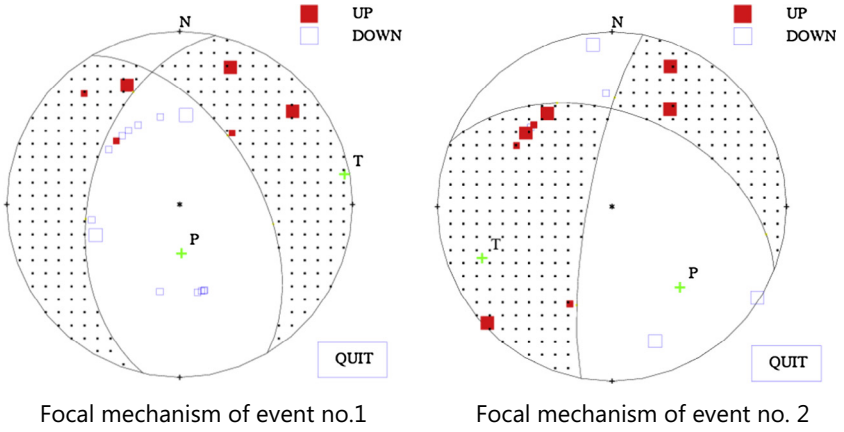

Figure 14 Diagrams of focal mechanism solutions of each event located at Sinai Peninsula.

Table 6 Parameters of the focal mechanisms used to evaluate stress tensor in northern Red Sea.

No.	Date			Time			Fault planes				Stress axes				Refs.
							NP1		NP2		*P*-axis		*T*-axis		
	Yr.	Mo.	Day	Ho.	Mn.	Sec.	St.1	Dip1	St.2	Dip2	Az.	Pl.	Az.	Pl.	
1	1969	3	31	7	15	54	294	37	113	53	19°	82°	203°	08°	Hu
2	1972	6	28	9	49	35	288	40	121	51	75°	82°	205°	05°	Hu
3	1994	9	26	17	27	6	321	89	53	40	264°	34°	19°	32°	
4	1994	11	4	6	0	48	323	88	58	30	261°	40°	28°	36°	
5	1995	4	20	10	41	53	126	78	229	43	74°	42°	186°	22°	
6	1996	5	29	21	42	49	241	58	138	71	95°	37°	192°	09°	
7	1996	8	18	9	29	1	141	73	247	48	94°	43°	199°	16°	
8	1996	12	17	7	21	20	242	73	144	65	105°	31°	12°	05°	
9	1997	6	9	15	21	2	265	75	149	32	142°	52°	16°	25°	
10	2003	03	30	04	43	02	184	81	296	23	117°	50°	256°	32°	M07
11	2003	07	12	09	22	09	298	65	39	27	229°	68°	20°	20°	M07
12	2003	12	10	21	22	12	146	30	338	61	63°	15°	262°	74°	M07
13	2004	4	27	11	20	40	121	52	269	42	89°	73°	197°	05°	TS
14	2005	5	4	19	47	15	352	83	92	39	297°	40°	53°	27°	TS
15	2005	10	28	17	0	9	284	41	164	67	117°	55°	229°	15°	TS
16	2005	11	11	15	33	8	196	25	316	77	200°	53°	63°	29°	TS
17	2006	4	6	10	58	12	144	50	292	45	120°	73°	218°	02°	TS
18	2008	3	20	9	6	33	151	63	29	44	12°	56°	266°	11°	TS
19	2008	5	4	1	8	15	354	77	86	80	310°	16°	220°	02°	TS
20	2008	5	24	0	37	53	316	84	50	60	269°	26°	07°	17°	TS

Hu: Huang and Solomon (1987), M07: Mahmoud (2007), TS: This Study.

Table 7 Stress tensor parameters of the northern Red Sea.

$\sigma 1$		$\sigma 2$		$\sigma 3$		*R*	ϕ
Az.	Pl.	Az.	Pl.	Az.	Pl.		
250°	71°	144°	05°	52°	18°	0.4	5.1

$\sigma 1$, $\sigma 2$, and $\sigma 3$ are the directions of the principles stress, Az: Azimuth, Pl: plunge, *R*: stress ratio, and *F*: the average of misfit angle.

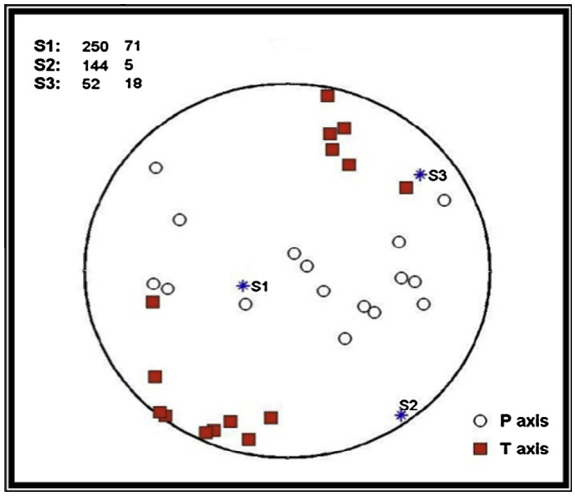

Figure 15 Results of stress tensor inversion of Northern Red Sea Zone showing the distribution of *P* and *T*-axes.

and minimum $\sigma 3$ stresses and hence constrains the shape of the stress ellipsoid.

The GF method proposed a grid search method of inverting focal mechanisms to obtain the stress tensor (focal mechanisms stress inversion, hence forward FMSI), in which stress field parameters are tried systematically against the focal mechanism orientations and the calculated misfit depending on the orientations of fault planes and slip directions indicated earthquake focal mechanisms.

A grid search over the focal sphere is performed at first with a 90° variance with 10° spacing (approximate method) then with a 30° variance and 5° spacing. Each inversion takes a significant amount of time to run, which depends mainly on the number of earthquakes to be inverted. The misfit of an individual fault-plane solution is the smallest rotation angle, about any axis, which brings the orientation of one of the observed fault planes, its slip vector and sense of slip in coincidence with the computed ones. The misfits of the slip vector in both nodal planes for all of the individual focal mechanisms are computed and from these, the average misfit is determined. We applied Gephart and Forsyth (GF) method on a set of synthetic focal mechanism, data sets *P* and *T* axes processed by FMSI, which inverts the focal mechanisms to obtain the stress tensor. The final stress model gives good indications about the preferred rupture direction that represents the most effective factors in performing the hazard assessment. In the following part we explain the calculated stress tensor for each seismic zone.

6.1. The northern Red Sea area

This seismic zone represented a broad area of active tectonics as evidenced by the high level of seismicity. Table 6 shows the parameters of the focal mechanisms used to evaluate stress tensor and the Stress inversion for focal mechanisms selected shows a relatively homogeneous stress pattern dominated by ENE-WSW (N52°E), extensional regime ($\sigma 3$ is more horizontal while $\sigma 1$ axis has steepest plunge) as shown in Table 7. Fig. 15 shows the distribution of *P*- and *T*-axes along northern

Table 8 Parameters of the focal mechanisms used to evaluate stress tensor in the Gulf of Suez.

No.	Date			Time			Fault planes				Stress axes				Refs.
							NP1		NP2		*P*-axis		*T*-axis		
	Yr.	Mo.	Day	Ho.	Mn.	Sec.	St.1	Dip1	St.2	Dip2	Az.	Pl.	Az.	Pl.	
1	1983	06	12	12	00	06	129	86	241	11	50°	48°	210°	40°	Ma
2	1992	10	27	09	04	46	171	51	312	46	146°	69°	242°	03°	A97
3	1992	10	27	11	02	44	158	66	271	49	116°	49°	218°	10°	CMT
4	1995	01	05	15	02	55	127	55	290	36	71°	77°	210°	09°	R
5	1995	02	09	15	52	46	161	54	309	41	124°	72°	237°	07°	R
6	1995	05	22	06	37	38	145	73	322	17	57°	62°	234°	28°	R
7	1995	08	04	21	50	34	143	66	313	24	61°	69°	230°	21°	R
8	1996	09	15	05	18	11	118	67	354	37	347°	57°	230°	17°	Ma
9	2000	05	09	18	43	32	144	77	243	57	98°	33°	197°	13°	ENSN
10	2000	11	03	21	19	03	117	41	297	49	207°	86°	27°	04°	ENSN
11	2003	01	06	12	35	26	15	52	113	80	342°	34°	239°	19°	ENSN
12	2003	01	15	11	31	28	307	51	151	42	159°	77°	48°	05°	ENSN
13	2003	03	03	08	56	48	194	30	60	02	257°	74°	96°	15°	M07
14	2003	03	23	13	21	49	321	36	76	73	309°	51°	190°	21°	M07
15	2003	04	01	15	34	42	385	67	159	31	329°	62°	99°	19°	M07
16	2003	04	23	10	37	13	316	62	74	48	277°	53°	18°	08°	M07
17	2003	09	09	08	39	00	337	75	75	64	293°	30°	28°	07°	M07
18	2003	12	30	14	56	11	153	57	294	40	113°	68°	226°	09°	M07
19	2004	07	06	12	13	12	325	44	135	47	334°	84°	230°	01°	TS
20	2004	08	16	22	42	50	279	72	168	42	148°	48°	36°	18°	TS
21	2004	11	28	21	50	04	310	65	130	25	220°	70°	40°	20°	TS
22	2005	12	08	01	28	11	281	43	151	59	112°	62°	219°	09°	TS
23	2006	09	28	06	32	12	308	53	87	45	278°	68°	19°	04°	TS
24	2008	01	25	03	19	42	304	30	171	69	113°	60°	245°	21°	TS
25	2008	03	14	03	52	37	143	46	294	48	133°	75°	38°	01°	TS

Ma: Maamoun et al. (1984), A97: Abdel Fattah et al. (1997), CMT: Centroid moment tensor solution published by ISC, R: Reda Abdel Fattah (2005), ENSN: Seismological bulletin published by Egyptian National Seismic Network.

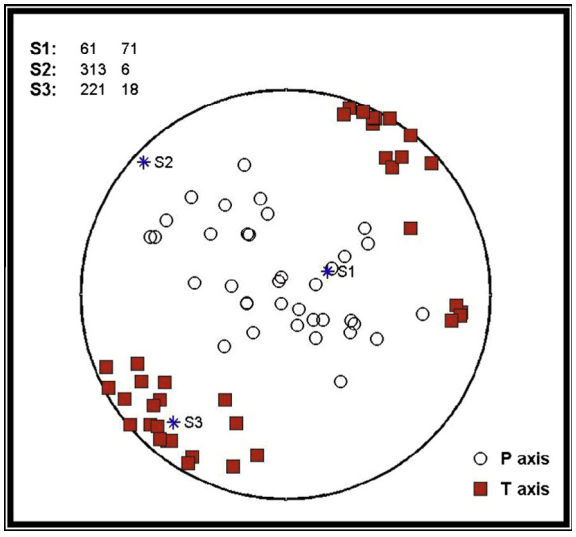

Figure 16 Results of stress tensor inversion of the Gulf of Suez showing the distribution of *P*- and *T*-axes.

Table 9 Stress tensor of the Gulf of Suez.

$\sigma 1$		$\sigma 2$		$\sigma 3$		R	ϕ
Az.	Pl.	Az.	Pl.	Az.	Pl.		
61°	71°	313°	06°	221°	18°	0.3	6.3

The referred symbols are the same as in pervious Tables.

Red Sea zone. The tension direction is nearly perpendicular to the Red Sea trend. These results are in good, consistent with Abou Elenean (1997) and Megahed (2004) which indicates that the tensional stress direction is N56°E(see Table 7).

Table 11 Stress tensor parameters of the Gulf of Aqaba.

$\sigma 1$		$\sigma 2$		$\sigma 3$		R	ϕ
Az.	Pl.	Az.	Pl.	Az.	Pl.		
329°	40°	133°	49°	232°	08°	0.3	−50

The referred symbols are the same as in pervious tables.

6.2. The Gulf of Suez

The focal mechanism solutions for earthquakes were used to calculate the stress tensor inversion in the Gulf of Suez (Table 8). The whole dataset shows that *P* axes cluster in the direction of WNW-ESE orientation and *T* axes are almost horizontal and trends in ~NE-SW (N41°E), as it is shown in Fig. 16. The inverse solution reflected a prevailed tension stress $\sigma 3$ that is trending NE-SW, while $\sigma 1$ is trending WNW-ESE. It shows a relatively homogeneous stress pattern which is nearly perpendicular to the rift trend. These results are in good consistent with Bosworth and Taviani (1996a,b) who came to a similar conclusion by analyzing borehole breakouts and mesoscopic faults arrays (N40°-45°E). This stress field leads to normal faulting NW-SE parallel to rift trend. The value of the best fitting stress models, the directions of $\sigma 1$, $\sigma 2$, $\sigma 3$, the stress ratio *R* value, and the value of the degree of misfit *F* are listed in Table 9.

6.3. The Gulf of Aqaba

The focal mechanism parameters of events used to evaluate the stress tensor presented in (Table 10).

The stress tensor inversion using GF method for the earthquakes fault plane solutions reflects the prevailed tension stress $\sigma 3$ trends N52°E back azimuth along the Gulf of Aqaba

Table 10 The focal mechanism parameters of events used to evaluate the stress tensor inversion in the Gulf of Aqaba.

No.	Date			Time			Fault planes				Stress axes				Refs.
							NP1		NP2		*P*-axis		*T*-axis		
	Yr.	Mo.	Day	Ho.	Mn.	Sec.	St.1	Dip1	St.2	Dip2	Az.	Pl.	Az.	Pl.	
1	1993	07	30	23	34	10	343	63	83	72	306°	33°	212°	06°	K98
2	1993	08	03	12	43	05	139	36	357	60	309°	67°	72°	13°	HRV
3	1993	08	03	16	33	21	328	67	67	70	288°	31°	197°	02°	K98
4	1993	08	07	04	55	40	348	60	86	76	311°	32°	214°	11°	K98
5	1993	08	20	23	09	59	350	63	89	73	312°	31°	218°	06°	K98
6	1993	10	18	20	51	14	74	80	339	61	300°	28°	203°	13°	K98
7	1993	11	03	18	39	32	324	69	75	47	280°	47°	25°	13°	K98
8	1993	11	08	01	06	02	350	60	93	69	314°	38°	220°	05°	K98
9	1993	12	04	23	34	11	331	54	95	52	302°	58°	34°	01°	K98
10	1995	11	22	04	15	11	196	59	294	77	159°	31°	62°	12°	PDE
11	1995	11	22	22	16	53	202	67	294	87	160°	18°	66°	14°	PDE
12	1995	11	23	18	07	17	199	77	108	83	154°	04°	63°	15°	PDE
13	1996	01	03	10	05	26	116	80	215	51	171°	19°	68°	35°	K98
14	2002	09	22	12	00	23	191	44	320	59	178°	61°	72°	08°	ENS
15	2005	01	20	13	41	50	41	43	178	56	120°	63°	50°	10°	TS
16	2008	02	03	17	06	46	58	75	156	62	171°	65°	60°	10°	TS
17	2008	04	04	14	05	20	146	46	287	51	132°	69°	36°	03°	TS
18	2008	04	04	14	14	48	145	46	294	49	135°	74°	39°	02°	TS

K98: Abou Elenean (2007), PDE: Solution by NEIS, HRV: Harvard CMT solutions.

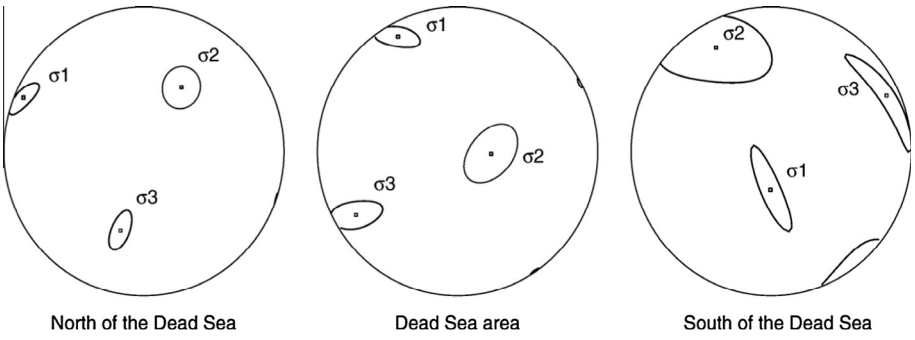

Figure 17 Representative stress tensor for Dead Sea region (Hofstetter et al., 2007).

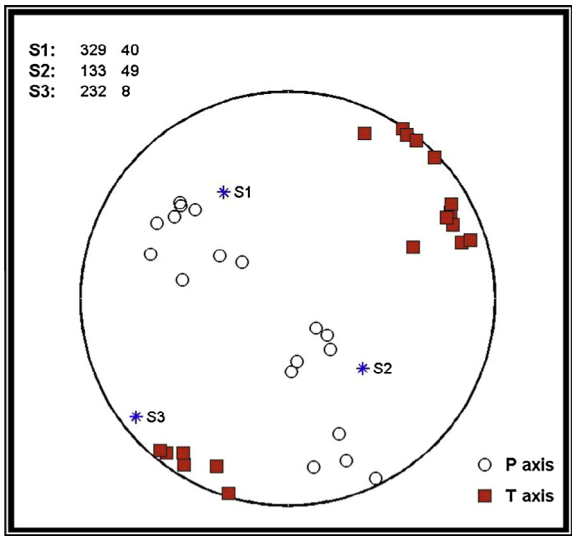

Figure 18 Results of stress tensor inversion of the Gulf of Aqaba.

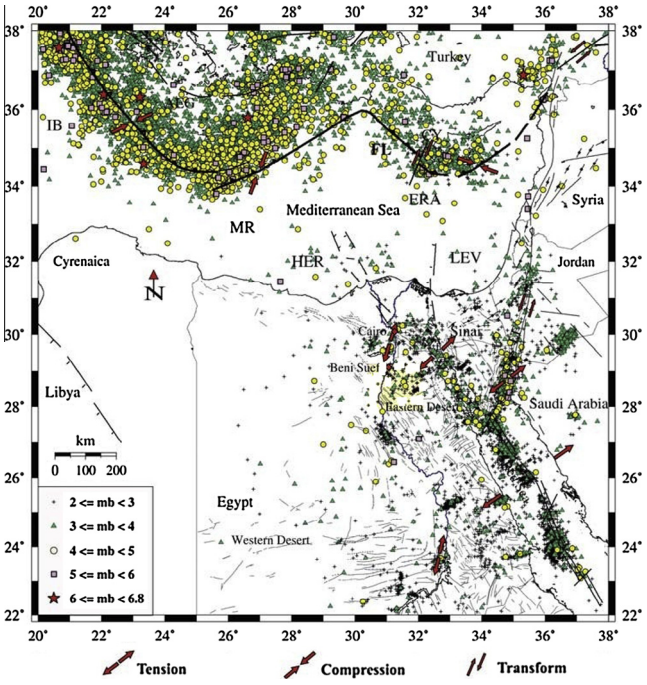

Figure 19 Tectonic boundaries of the Eastern Mediterranean Region, and Stress directions in Egypt. Seismicity data ($2 \leqslant mb < 6.8$) were compiled after ENSN and NEIC from 1997 to 2007. (Compiled by Abou Elenean and Hussein (2008)). Acronyms represent: AEG – Aegean Sea; CY – Cyprus; ERA – Eratosthenes Seamount; FL – Florence; IB – Ionian Basin; MR – Mediterranean Ridge; LEV – Levantine Basin; LF – Levant Fault; ROS – Rosetta; QAT – Qattara; TEM – Temsah; MS – Misfak; BAR – Bardawil.

(Table 11) due to the fact that $\sigma 1$ is vertical in the regional inversions. So, this stress field leads to left lateral strike slip movement with normal component. This extension trend is in a good agreement with a closer extension trend (N53°E) in the same area that was deduced from inversion of 14 earthquake mechanisms (Abou Elenean, 1997). Also, it shows good agreement with the paleo-stress measurements along the Gulf of Aqaba that supports the idea of the recent reactivation of Oligocene–Miocene stress cycle, and a rotation of the regional stress pattern in the vicinity of the transform fault (see Table 10 and Table 11).

The results of the stress direction along the Dead Sea fault have two directions dominated the fault plane population (Hofstetter et al., 2007) Fig. 17. The first cluster has an azimuth close to N15°, which corresponds to the overall direction of the Dead Sea fault (DSF). The second cluster is closer to N120°, corresponding to the direction of the Carmel–Gilboa fault system and they noted that seismicity in the Dead Sea basin is strongly dominated by strike–slip mechanisms, from which a large part has a fault plane oriented perpendicular to the longest axis of the basin, rather than by normal faulting. It is fully consistent with the pull-apart hypothesis of the Dead Sea basin controlled by strike–slip motion along the DSF comparative with our results is that the Gulf of Aqaba has different stress direction rather than the results of (Hofstetter et al., 2007) that is the prevailed stress direction is N52°E as shown in Fig. 18.

7. Correlation of results with previous studies

From the present study and the previous we note that the stress pattern changes by time. Specially Gulf of Suez indicates that the prevailed stress (Azimuth) is decreased from 46° to 41° corresponding to the Arabian Plate motion in NE as shown in Figs. 19 and 20 respectively. A left lateral fault boundary with

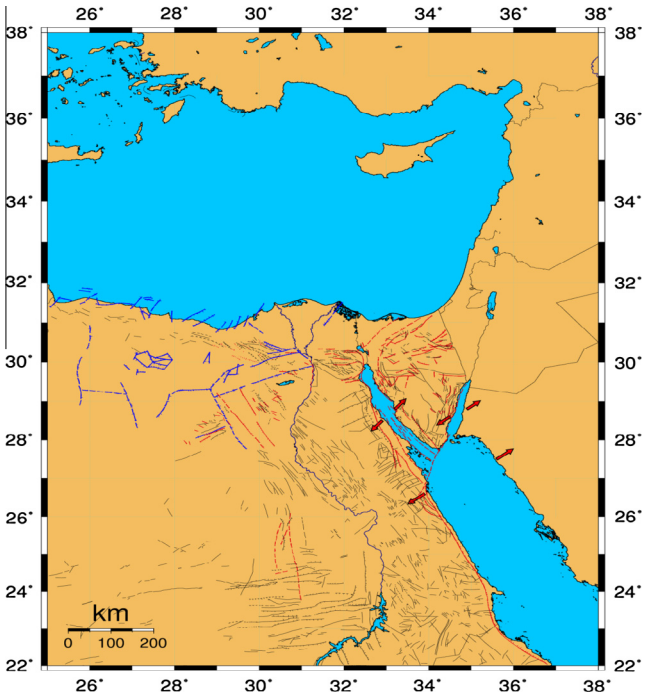

Figure 20 Recent stress tensor for the study area modified after (Abou Elenean and Hussein, 2008).

the African Plate called the Dead Sea Transform (DST), and a divergent boundary with the African Plate called the Red Sea Rift run the length of the Red Sea. Regarding the study presented by Hussein et al. (2013) we note that the stress direction pattern is decreased from 44° to 41° and from 56° to 52° at Gulf of Suez and Gulf of Aqaba respectively corresponding to the Arabian Plate motion in the Northern East direction.

Correlation between our results about stress field pattern and published studies for this area.

Zone	$\sigma 1$		$\sigma 2$		$\sigma 3$		R	ϕ
	Az.	Pl.	Az.	Pl.	Az.	Pl.		
Abou Elenean (1997)								
N-Red Sea	203°	59°	318°	15°	56°	27°	0.3	5.6
Gulf of Suez	105°	39°	341°	34°	226°	32°	0.5	3.5
Gulf of Aqaba	333°	27°	114°	56°	233°	18°	0.3	2.7
Mahmoud (2007)								
N-Red Sea	155°	59°	314°	29°	49°	09°	0.5	4.7
S-Gulf of Suez	216°	76°	313°	02°	43°	14°	0.4	5.8
Gulf of Aqaba	265°	70°	140°	12°	47°	16°	0.5	1.27
Hussein et al. (2013)								
N-Gulf of Suez	86	77	308	09	216	08	0.55	0.51
S-Gulf of Suez (A)	275	85	135	04	44	03	0.62	7.58
S-Gulf of Suez (B)	250	67	40	20	134	11	0.47	11.74
Gulf of Aqaba (A)	325	19	147	71	56	01	0.69	6.67
Gulf of Aqaba (B)	184	09	07	81	274	01	0.44	9.01
This Study								
N-Red Sea	250°	71°	144°	05°	52°	18°	0.4	5.1
Gulf of Suez	61°	71°	313°	06°	221°	18°	0.3	6.3
Gulf of Aqaba	329°	40°	133°	49°	232°	08°	0.3	5.0

8. Conclusions

There are three seismic zones affected the northeastern part of Egypt; the Northern Red Sea, Gulf of Suez and Gulf of Aqaba. The focal mechanism solutions were carried out for 24 events recorded by the Egyptian National Seismic Network (ENSN) during the period from 2004 to 2008. These solutions were obtained with high reliability based on polarity of P-wave first motion by the applied (Suetsugu, 1995) method. The focal mechanisms deduced in this study indicated a dominant tension stress along the NE African corner. The tension axis trends ENE-WSW along the Gulf of Suez, Gulf of Aqaba and northern Red Sea, take NNE-SSW trends toward the land. The results demonstrate mainly a normal faulting, pure extension, with strike slip extension. Focal mechanism solutions of some events illustrate the existence of strike-slip mechanism. These results indicate that Egypt is dominated by three groups of neotectonic regimes. They are the extensional tectonic regime, normal to strike slip regime and strike-slip tectonic regime.

This study asserts a dominant extension without any indication of compressive stress on land or along the Northern Red Sea–Gulf of Suez rifts which is consistent with that of Lyberis (1988) and Bosworth and Taviani (1996a,b). The Results of the stress tensor using focal mechanisms of recent earthquakes indicate a prevailed tension, stress field in northern Red Sea is N52°E, the Gulf of Suez is 41°, and the Gulf of Aqaba is 52° these results are consistent within situ for each zone and field studies related to Lyberis (1988) and Bayer et al. (1988).

Acknowledgments

The authors are grateful to Dr. Gephart and Forsyth (1984) for supporting us with their software. The authors would like to express their deep thanks to the staff of the Egyptian National Seismic Network for providing us with valuable data. The authors are also grateful to the reviewers for their constructive comments.

References

Abdel Aal, Price, J., Vaitl, D.J., Shrallow, A., 1994. Tectonic evolution of the Nile Delta impact on sedimentation and hydrocarbon. In: Twelfth Petroleum Exploration and Production Conference, November 1994, pp. 19–34.

Abdel Fattah, R., 2005. Seismotectonics of Sinai Peninsula, Egypt and their implications for seismic hazard evaluation. Ph.D. Thesis, Fac. of Sci., Geol. Dept. Mansoura Univ., Egypt, pp. 224.

Abdel Fattah, A.K., Hussein, H.M., Ibrahim, E.M., Abu El Atta, A.S., 1997. Fault plane solutions of the 1993 and 1995 Gulf of Aqaba earthquakes and their tectonic implications. Annali di Geofisica 40, 1555–1564.

Abdel Fattah, A.K., Hussein, H.M., El Hady, S., 2006. Another look at the 1993 and 1995 Gulf of Aqaba earthquake from the analysis of teleseismic waveforms. Acta Geophys. 54 (3), 260–279.

Abou Elenean, K.M., 1997. Seismotectonics of Egypt in relation to the Mediterranean and Red Sea tectonics. Ph.D. Thesis, Fac. Sci. Ain Shams Univ., Egypt.

Abou Elenean, K.M., 2007. Focal mechanisms of small and moderate size earthquakes recorded by the Egyptian National Seismic Network (ENSN), Egypt. NRIAG J. Geophys. 6 (1), 117–151.

Abou Elenean, K.M., Hussein, H.M., 2008. The October 11, 1999 and November 08, 2006 Beni Suef Earthquakes, Egypt. Pure Appl. Geophys. 165 (7), 1391–1410. http://dx.doi.org/10.1007/s00024-008-363-3.

Ambraseys, N.N., Melville, C.P., Adams, R.D., 1994. The Seismicity of Egypt, Arabia and Red Sea. Cambridge University Press, Cambridge.

Bayer, H.J., Hötzl, H., Jado, A.R., Roscher, B., Voggenreiter, W., 1988. Sedimentary and structural evolution of the northwest Arabian Red Sea margin. Tectonophysics 153 (1–4), 137–151.

Ben-Menahem, A., Aboodi, E., 1971. Tectonic patterns in the Red Sea region. J. Geophys. Res. 76, 2674–2689.

Ben-Menahem, A., Nur, A., Vered, M., 1976. Tectonics, seismicity and structure of the Afro-Euroasian junction – the breaking of an incoherent plate. Phys. Earth Planet. Inter. 12, 1–50.

Bosworth, W., Taviani, M., 1996a. Seismological observations in and around the Southern Part of the Gulf of Suez, Egypt. Bulletin of the Seismological Society of America 91, 708–717.

Bosworth, W., Taviani, M., 1996b. Late Quaternary reorientation of stress field and the extension direction in the southern Gulf of Suez, Egypt: Evidence from uplifted coral terraces, mesoscopic fault arrays and borehole breakouts. Tectonics 15, 791–802.

Chenet, P., Colletta, B., Letouzey, J., Desforges, G., Ousset, E., Zaghloul, E.A., 1985. DÈcollement and extensional tectonics on the eastern margin of the Suez rift. In: Symposium on Continental Extensional Tectonics, University of Durham, 1985, Abstr. 24.

Courtillot, V., Armijo, R., Tapponier, P., 1987. The Sinai junction revisited. Tectonophysics 141, 181–190.

De Vicente, G., Olaiz, A., Muñoz-Martín, A., Vegas, R., Cloetingh, S., Galindo, J., Rueda, J., A lvarez., J., 2006. Campo de esfuerzos activo entre Iberia y Argelia. Inversión de mecanismos focales del tensor del momento sísmico. In: paper presented at 5th Asamblea Hispano Portuguesa de Geodesia y Geofísica, Com. Española de Geod. y Geofís., Seville, Spain.

Egyptian Geological Survey and Mining Authority, EGSMA, 1981. Geologic Map of Egypt, 1:2000000.

Egyptian National Seismic network (ENSN) Bulletin (1997-2009). Earthquakes in and around Egypt. NRIAG J. Geophys. 6 (1), 119–153.

El-Hadidy, S., 1995. Crustal structure and its related causative tectonics in northern Egypt using geophysical data. Ph.D. Thesis. Ain Shams Univ.

Eyal, M., Eyal, Y., Bartov, Y., Steinitz, G., 1981. The tectonic development of the western margin of the Gulf of Aqaba rift. Tectonophysics 80, 39–66.

Garfunkel, Z., Bartov, Y., 1977. The tectonics of the Suez Rift. Bull. Geol. Surv. Isr. 71, 1–44.

Garfunkel, Z., Ben-Avraham, Z., 1996. The structure of the Dead Sea Basin. Tectonophysics 266, 155–176.

Gephart, J., Forsyth, W., 1984. An improved method for determining the regional stress tensor using earthquake focal mechanism data: application to the San Fernando Earthquake Sequence. J. Geophys. Res. 89, 9305–9320.

Gergawi, A., El-Khashab, H.M.A., 1968. Seismicity of Egypt. Helwan Observatory Bull. 76.

Halsey, G.H., Gardner, W.C., 1975. Tectonic Analysis of Egypt using ERTS-1 Satellite Data: A Lecture Delivered at the General Petroleum Company of Egypt, Cairo.

Hofstetter, A., Thio, H.K., Shamir, G., 2003. Source mechanism the 22/11/1995 Gulf of Aqaba earthquake and its aftershock sequence. J. Seismol. 7, 99–114.

Hofstetter, R., Klinger, Y., Abdel-Qader, A., Rivera, L., Dorbath, L., 2007. Stress tensor and focal mechanisms along the Dead Sea Fault and related structural elements based on seismological data. Tectonophysics 429, 165–181.

Huang, P.Y., Solomon, S.C., 1987. Centroid depths and mechanisms of midocean ridge earthquakes in the Indian Ocean, Gulf of Aden and Red Sea. J. Geophys. Res. 92, 1361–1382.

Hussein, H.M. et al, 2013. Present-day tectonic regime in Egypt and surrounding area based on earthquake focal mechanisms. J. Afr. Earth Sci. 81, 1–13.

Ismail, A., 1960. Near and local earthquakes at Helwan from 1903–1950. Helwan Observatory Bull. 49.

Kebeasy, R.M., 1990. Seismicity. In: Said, R. (Ed.), Geology of Egypt. A. Balkerma, Rotterdam, pp. 51–59.

Khattri, K., 1973. Earthquake focal mechanism studies – a review. Earth Sci. Rev. 9, 19–63.

Kisslinger, C., Bowman, J.R., Koch, K., 1981. Procedures for computing focal mechanisms from local (SV/P) data. Bull. Seismol. Soc. Am. 71, 1719–1729.

Klinger, Y., Rivera, L., Haessler, H., Maurin, J.C., 1999. Active faulting in the Gulf of Aqaba: new knowledge from the MW 7.3 earthquake of 22 November 1995. Bull. Seismol. Soc. Am. 89, 1025–1036.

Lund, B., Slunga, R., 1999. Stress tensor inversion using detailed micro earthquake information and stability constraints: applications to Olfus in southwest Iceland. J. Geophys. Res. 104, 14947–14964.

Lyberis, 1988. Tectonic evolution of the Gulf of Suez and Gulf of Aqaba. Tectonophysics 153, 209–220.

Maamoun, M., Allam, A., Megahed, A., Abu El- Ata, A., 1980. Neotectonics and seismic regionalization of Egypt. Bull. Inter. Ins. Seism. Earthquake Eng. (BIISEE) 18, 27–39.

Maamoun, M., Megahed, A., Allam, A., 1984. Seismicity Egypt. Helwan Inst. Astron. Geophys. Bull. 4, Ser..

Marzouk, I., 1988. Study of crustal structure of Egypt deduced from deep seismic and gravity data. Ph.D. Institute of Geophysics, University of Hamburg.

Megahed, A., 2004. Seismic deformation studies on the northeastern part of Egypt. Ph.D. Thesis. Fac. of Sci., Geology Dept. Mansoura Univ.

Mahmoud, S.H., 2007. Seismotectonics of Sinai peninsula and surrounding area. Ph. D. Thesis. Fac. of Sci., Geophysics Dept., Ain Shams Univ.

Meshref, W., 1982. Regional structural setting of Northern Egypt. In: Proceedings of the 6th Exploration Seminar, EGPC, Cario, pp. 1734.

Meshref, W., 1990. Tectonic framework. In: Said, R. (Ed.), The geology of Egypt. A.A Balkema, Rotterdam, Netherlands, pp. 113–155.

Mosconi, A., Rebora, A., Venturino, G., Bocc, P., Khalil, M.H., 1996. Egypt-Nile Delta and North Sinai Cenozoic tectonic evolutionary model: a proposal. In: Proc. of the 13th Egypt Gen. Petrol. Corp. Explor. And Prod. Conference, Cairo, Egypt, vol. I, pp. 203–223.

Moustafa, A., Abd-Allah, A., 1992. Transfer zones with en echelon faulting at the northern end of the Suez rift. Tectonics 11 (3), 499–509.

Moustafa, A., 2002. Controls on the geometry of transfer zones in the Suez rift and northwest Red Sea: implications for the structural geometry of rift systems. AAPG Bull. 86, 979–1002.

Pinar, A., Türkelli, N., 1997. Source inversion of the 1993 and 1995: Gulf of Aqaba earthquakes. Tectonophysics 283, 279–288.

Sieberg, A., (1932). Untersuchungen ueber Erdbeben und Bruchschollenba im Oestlichen Mittelrmeergebiet, Denkschriften dermed, naturw, Ges. Zu Jena, 18- band, 2. Lief.

Stein, S., Wysession, M., 2003. An Introduction to Seismology, Earthquakes, and Earth Structure. Blackwell Publishing.

Suetsugu, D., 1995. Earthquakes Source Mechanism. International Institute of Seismology and Earthquake Engineering (IISEE), Building Research Institute, Japan.

Tapponnier, P., Armijo, R., 1985. Seismotectonics of Northern Egypt. Terra Cognita 5, 171, abstract.

Youssef, M.I., 1968. Structural pattern of Egypt and its interpretations. AAPG Bull. 52 (1968), 601–614.